Inkjet-printed embedded Ag-PEDOT:PSS electrodes with improved light out coupling effects for highly efficient ITO-free blue polymer light emitting diodes

Lukas Kinner, Sebastian Nau, Karl Popovic, Stefan Sax, Ignasi Burgués-Ceballos, Felix Hermerschmidt, Alexander Lange, Christine Boeffel, Stelios A. Choulis, and Emil J. W. List-Kratochvil

Citation: Appl. Phys. Lett. **110**, 101107 (2017); doi: 10.1063/1.4978429

View online: http://dx.doi.org/10.1063/1.4978429

View Table of Contents: http://aip.scitation.org/toc/apl/110/10

Published by the American Institute of Physics

Inkjet-printed embedded Ag-PEDOT:PSS electrodes with improved light out coupling effects for highly efficient ITO-free blue polymer light emitting diodes

Lukas Kinner,[1,a)] Sebastian Nau,[1] Karl Popovic,[1] Stefan Sax,[1] Ignasi Burgués-Ceballos,[2] Felix Hermerschmidt,[2] Alexander Lange,[3] Christine Boeffel,[3] Stelios A. Choulis,[2] and Emil J. W. List-Kratochvil[4,a)]

[1]*NanoTecCenter Weiz Forschungsgesellschaft mbH, Franz-Pichler-Straße 32, 8160 Weiz, Austria*
[2]*Molecular Electronics and Photonics Research Unit, Department of Mechanical Engineering and Materials Science and Engineering, Cyprus University of Technology, 45 Kitiou Kyprianou Street, 3041 Limassol, Cyprus*
[3]*Fraunhofer Institute for Applied Polymer Research, Geiselbergstraße 69, 14476 Potsdam-Golm, Germany*
[4]*Institut für Physik, Institut für Chemie & IRIS Adlershof, Humboldt-Universität zu Berlin, Brook-Taylor-Straße 6, 12489 Berlin, Germany*

(Received 29 November 2016; accepted 27 February 2017; published online 10 March 2017)

We report on solution processed polymer light emitting diodes (PLEDs) using inkjet-printed embedded and non-embedded metal grid anodes. Metal grids were inkjet-printed in a honeycomb layout. Honeycomb dimensions were varied from 3 mm to 8 mm to optimize device performance. Inkjet-printed grids were then coated with a highly conductive PEDOT:PSS formulation. First experiments on PEDOT:PSS coated, non-embedded metal grid anodes showed that grids with a 3 mm honeycomb diameter have a similar efficiency as optimized indium tin oxide (ITO) based reference devices. To further improve the efficiency of the devices, the honeycomb Ag-grids were embedded in an Ormocer®-based material. A detailed performance analysis of PLEDs fabricated on ITO, non-embedded and embedded grids was carried out. It is shown that reduced leakage current and enhanced light outcoupling by embedding result in a significant efficiency enhancement of 250% in inkjet-printed embedded Ag-PEDOT:PSS ITO-free PLEDs, compared to the ITO-based reference PLEDs. *Published by AIP Publishing.* [http://dx.doi.org/10.1063/1.4978429]

With the demonstration of electroluminescence from organic materials, an unprecedented development of organic light emitting diodes (OLED) was put into place.[1,2] Although still expensive, they have made their way into everyday life as displays in smartphones or flat-screen TVs. Because of high costs, lighting applications are currently mostly found in a premium and design lamp sector. In contrast to spot light sources (e.g., inorganic LEDs), OLEDs can be realized as area light sources with essentially no limits to size and design.[3]

A serious constraint, however, is given by the significant series resistance values of indium tin oxide (ITO) and the most commonly used transparent conductive electrode (TCE), leading to a large voltage drop resulting in a luminance gradient towards the center of a lighting panel.[4] Moreover the brittleness of ITO significantly hampers the development of flexible and conformable OLED applications. Numerous technologies have been put forward to overcome these issues, including different transparent conductive oxides (TCOs), Ag-nanowires,[5–8] supportive metal electrodes,[9–13] etc. There are several reports of the realization of such supportive metal electrodes, either applied on ITO or with a covering of a conductive poly(3,4-ethylenedioxythiophene) polystyrene sulfonate (PEDOT:PSS) layer.[14–17] Furthermore, it has been shown that structured metal lines and PEDOT:PSS films show a higher stability against mechanical stress and bending.[18–20]

However, in most cases, these electrodes have been structured and deposited by rather costly photolithographic means. An alternative is represented by economically and ecologically viable printing methods. Selective drop-on-demand inkjet-printing (IJP) allows for direct material deposition, low processing temperatures, and flexible, digital computer aided design-based production, which also delivers high enough resolutions for TCEs in lighting applications.[21] Special printing technologies, e.g., electro hydrodynamic nanodrip printing, could deliver high enough resolutions to print highly transparent and conductive metal electrodes for the use in displays, but the feature height of sufficiently conducting structures are still in the range of IJP patterns (400–800 nm).[22]

Generally, when using IJP bottom electrodes, the typical feature height of printed structures of several 100 nm turns out to be a serious issue, as they are in the thickness range, of the active layer stack, of a typical organic device. Moreover, printed structures tend to exhibit a rough surface with many spikes or defects after the thermal or photonic sintering of the metal precursor. A complete and defect-free covering by the subsequent organic layers is usually challenging, when processed from solution, leading to shorts in the device and/or high leakage currents. In thin film devices, electric fields at spikes and bumps are higher than in homogeneous layers; therefore, OLEDs as bias driven devices show local electrical break downs at inhomogeneities in the layers. Although we have previously shown that a reduction of the printed line height to <100 nm in non-embedded

[a)]Authors to whom correspondence should be addressed. Electronic addresses: lukas.kinner@ait.ac.at and emil.list-kratochvil@hu-berlin.de

inkjet printed metal grids is possible,[23] this typically leads to a reduction of the current carrying capacity of the grid lines. Creating a sufficient conducting cross section could also be achieved by increasing the line width, but this influences the transmission negatively. The embedding process for IJP ITO-free electrodes was previously proposed and developed for organic photovoltaics (OPVs).[24] While OPV devices do not necessarily need a flat electrode surface for charge carrier collection, achieving intimate surface and interfaces, it is far more crucial for OLEDs. A high-performance OLED device demands a flat and smooth electrode surface, to achieve homogeneous electric fields, charge carrier injection, and resulting homogenous light emission.

To address these issues, we report on polymer light emitting diodes (PLEDs), based on IJP embedded and non-embedded metal-grid/PEDOT:PSS electrodes. A supportive Ag-grid was inkjet printed in a honeycomb layout, using commercial nanoparticle based Ag-ink. The structure was embedded in an Ormocer®-material to overcome the unfavorable height and roughness of the printed structure.

IJP lines are not only embedded but also transferred and flipped so that the lines are turned upside down after printing. Hence, the whole electrode configuration is planarized and promotes a flattened surface compared to non-embedded lines. Because of the transfer, the ink can be printed on virtually any substrate, e.g., glass or PET, and then be transferred to any other substrate, e.g., glass or Polyethylene terephthalate (PET). Highly conductive (HC) PEDOT:PSS was used as an electrode and applied on the grid structure. It will be shown later in the text that such a configuration has device efficiencies significantly higher compared to ITO devices, since embedding reduces leakage currents and significantly improves light outcoupling. The proposed IJP embedded metal grid anode stack can, therefore, provide a serious, easily applicable and low-cost ITO-free electrode.

In a first step, Ag-nano particle ink was IJP in a honeycomb layout with a PixDro LP50 printer equipped with a FujiFilm Dimatix (Spectra) S-Class 128 nozzle piezoelectric print head. IJP grids were over coated with Clevios F CE (F CE) via conventional spin coating. F CE, a commercially available ready-to-use formulation of HC PEDOT:PSS, is specially designed for over coating of high and rough structures. Subsequently, poly(indenofluorene)-triphenylamine co-polymer was applied as hole injection layer (HIL). A poly(indenofluorene)-based co-polymer was used as the light emitting polymer (LEP). Details of the materials and processing are reported elsewhere.[25] Ca and Al were used as the top electrode.

Figure 1(a) shows the schematic representation of our PLED stack with IJP non-embedded Ag-lines. The line height and layer thicknesses were measured with a Dektak stylus profilometer (for details, see Figures S1–S4 of supplementary material). Subsequent to printing the grid structure, a layer of F CE was spin coated over the lines, followed by the other layers of the stack. Line heights of up to 800 nm were obtained. Because of these high lines, a conformal propagation of the line profile, as schematically shown in Figure 1(a), was found. The induced bumps and peaks in the topography lead to a low device yield, caused by shorts through the layers or at least high parasitic dark currents through the thinner material layers. One possible solution to overcome these undesired effects would be a thicker layer of PEDOT:PSS F CE, which, however, leads to an increased series resistance and a lower device efficiency.

Embedding the grid lines allow to apply a thinner F CE layer on a pre-flattened, planarized surface, lowering spikes, and hence, a reduced risk of creating defects and shorts through the active layers of the PLED, by providing good transparency. Figure 1(b) shows the schematic representation of such an embedded Ag-grid/PEDOT:PSS electrode stack. Although embedded, the lines (600–800 nm height) still tower 100–200 nm above the Ormocomp® layer. With an approximately 300 nm thick F CE layer the lines were fully covered, and a sufficiently flat electrode for applying the remaining PLED layers was achieved. Such embedded grid/PEDOT:PSS electrodes were then compared to conventional ITO-based and non-embedded reference electrode stacks.

For the grids in this study, a honeycomb layout was chosen, as it provides the best balance between lowest possible coverage (i.e., shadowing) and a sufficient and homogeneous

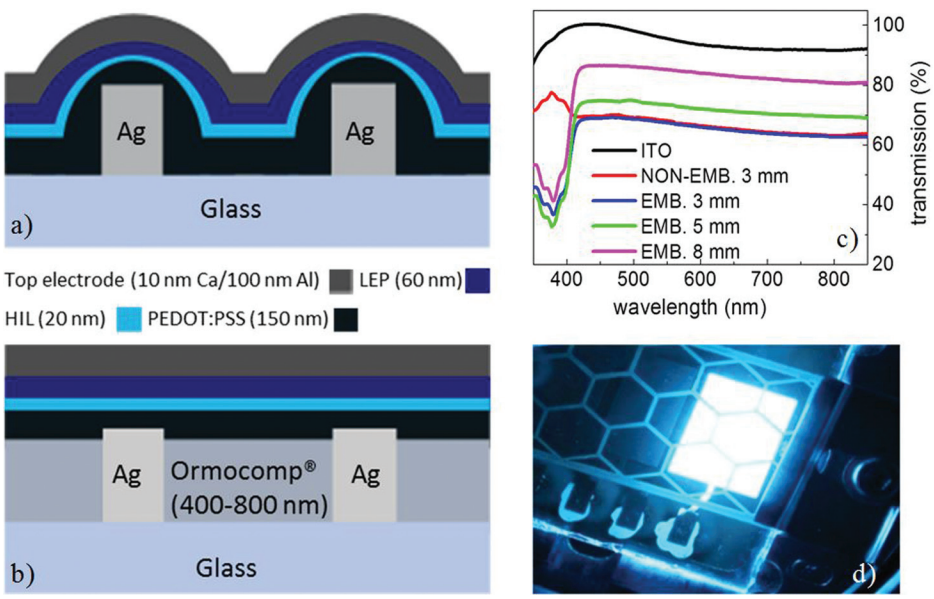

FIG. 1. Schematic representation of the PLED stack with non-embedded Ag-ink lines (a); schematic representation of PLED stack with embedded grid lines (b); transmission of the tested electrode stacks (c); and operating PLED (embedded 5 mm grid/PEDOT:PSS electrode) (d).

distributed number of conductive paths, compared to other geometries such as triangles, rectangles, or parallel lines. Honeycombs with different diameters (spacings) were printed on glass substrates to evaluate the optical transmission, as this parameter is an essential demand to a serious competitor to established technologies. Since grids have areas with 100% transmission in between and areas with zero transmission behind grid lines, these measurements can be interpreted as average transmissions of the corresponding grid sizes, not the device light out-coupling factors. Benchmarked against ITO, IJP Ag-grids with diameters of 8 mm and a line width of 350 μm already have a comparable transmission in the relevant optical range (Figure S5 of supplementary material).

In this study, five different electrode stacks are compared. A standard ITO/PEDOT:PSS-AL4083 electrode (ITO) was used as a reference device. Additionally, a 3 mm grid covered with F CE (non-embedded) and 3 mm, 5 mm, and 8 mm grids embedded in Ormocomp® and coated with F CE were compared. Devices using only F CE as electrode had a too high fault rate and were, therefore, excluded. Figure 1(c) shows the transmission of the compared electrode systems. ITO covered with PEDOT:PSS displays a transmission of up to 98%, while the 3 mm grid/PEDOT:PSS electrode shows a transmission of up to 70%. Embedded and non-embedded 3 mm grids only differ for wavelengths <400 nm which is caused by the Ormocomp® layer. Larger grid spacings show higher transmissions: The 5 mm grid/PEDOT:PSS electrode exhibits a transmission of up to 75% and the 8 mm grid/PEDOT:PSS electrode stack has a transmission of up to 85%. It is important to mention that the transmission values of the grids differ between Figures 1(c) and S5 (supplementary material) (due to different PEDOT:PSS-formulations) as the F CE layer (300 nm) covering the grids was five times thicker as the AL4083 layer (60 nm) on the ITO substrate; therefore, the entire grid electrode stacks show a lower transmission than the pure grids. Furthermore, it is important to mention that the transmission values of the grids are related to an average shadowing of the grid and not to a device dependent light out-coupling. Due to the favorable transmission properties of Ormocomp® (for the visible spectral range Ormocomp® shows a transmission of approximately 97%.), there are no significant differences in transmission between embedded and non-embedded Ag-grids. Ag-grids show wavelength independent constant values over the whole measured spectral range. This is caused by the fact that the printed geometries are by far too thick to reveal material dependent transmission properties. Figure 1(d) shows an image of a working 5 mm honeycomb-diameter grid/PEDOT:PSS electrode device. Although the material is a deep blue emitter, the color of the light seems to be white due to the high brightness.

As discussed previously, not only the transmission of the anode is important for its usage in a PLED device. The electric performance also needs to be analyzed. Investigations of the electrode systems under study were performed via measuring current-voltage and luminescence-voltage characteristics, followed by analyzing the efficiencies of the used PLED stack.

Figure 2(a) shows the achieved luminescence characteristics (for the spectra, see Figures S6–S9 of supplementary material) of the described PLEDs on different electrode systems. PLEDs based on the ITO reference electrode achieve a

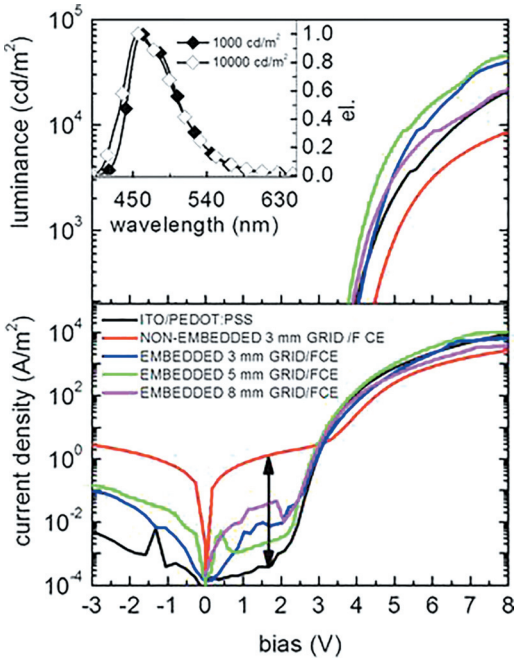

FIG. 2. Luminance characteristics of PLEDs on examined electrode structures (a) and current densities of PLEDs on examined electrode stacks (b).

luminance of maximum 20 000 cd/m^2, while PLEDs with the non-embedded 3 mm grid/PEDOT:PSS electrode have a luminance of maximum 9000 cd/m^2. PLEDs on embedded 3 and 5 mm grid/PEDOT:PSS electrodes achieve almost the same maximum luminance of 40 000 cd/m^2 and 42 000 cd/m^2. The 8 mm grid/PEDOT:PSS shows a luminance of maximum 20 000 cd/m^2. The inset of Figure 2(a) shows the normalized electroluminescence spectra of the light emitting polymer on an 8 mm grid/PEDOT:PSS electrode which is similar to the spectrum on the ITO/PEDOT:PSS electrode.

Simultaneous to luminance, current-voltage characteristics were measured. Figure 2(b) shows the corresponding current densities to the achieved luminance values. The ITO devices exhibit the lowest leakage current. The leakage current of the devices on the non-embedded grid/PEDOT:PSS electrodes are almost 4 orders of magnitude higher than that on the other electrodes (black arrow). Importantly, after embedding the devices show 400 times lower leakage currents than those based on non-embedded grids, but still one order of magnitude higher leakage currents compared to ITO-based reference devices. This is expected as ITO features the flattest electrode system, hence provides the lowest possibility of shorts. The current density of the PLED on 8 mm embedded grid/PEDOT:PSS electrode displays the lowest values of the grid-based devices in terms of leakage current. These above performance values are also summarized in Table I.

Exact sheet resistance estimations of IJP-grids are difficult to determine due to the previously discussed grid properties. Transmission measurements on their own do not depict sufficient quality standards of the grids, due to differences in the sequence of refractive indices between measurement and in the device. To compare the quality of our electrode stacks, the efficiency plotted versus the luminance is the most reliable data.

Figure 3 shows the efficiencies of PLEDs on an ITO reference electrode, 3 mm non-embedded and 3 mm, 5 mm, 8 mm embedded grid/PEDOT:PSS electrodes. The efficiency

TABLE I. Summary of basic data of compared electrode stacks.

Grid structure	Max. efficiency [cd/A]	Efficiency [cd/A][a]	Max. luminance [cd/m^2]	Luminance [cd/m^2][b]
ITO	3.7	2.8	20 000	5400
Spacing: 3 mm width: 150 μm non-embedded	3.4	3.1	9000	7100
Spacing: 3 mm width: 150 μm embedded	7	5.2	40 000	13 000
Spacing: 5 mm width: 150 μm embedded	6.4	4.9	42 000	12 000
Spacing: 8 mm width: 150 μm embedded	9.4	6	20 000	11 000

[a]Measured at 1000 cd.
[b]Measured at 2000 A/m^2.

is plotted versus luminance. Although the ITO electrode exhibits a measured transmission of up to 98%, its efficiency is the lowest with only up to 3.4 cd/A. By replacing ITO with a non-embedded 3 mm grid/PEDOT:PSS electrode, devices have low yield, but for the limited amount of the ones that can work, this efficiency value is exceeded with a maximum of 3.7 cd/A achieved. At a current density of 6500 A/m^2, the ITO device shows 13 000 cd/m^2 and the non-embedded 3 mm grid/PEDOT:PSS device exhibits 12 000 cd/m^2. Therefore, the 3 mm non-embedded grid/PEDOT:PSS devices reach similar luminescence values as the ITO reference at constant current.

While some parts of the light are fully blocked by the grid, overall, due to higher light out-coupling from the PEDOT:PSS-only/glass compared to the PEDOT:PSS/ITO/glass interface,[26–28] more light gets out of the ITO-free device at lower currents, resulting in a higher current efficiency. The work by Sun and Forrest has shown that 60%–80% of the light generated in an OLED is trapped, because of the worse refractive index matching of ITO ($n = 2.10$ at 450 nm) between organic materials ($n \approx 1.75$) and glass ($n = 1.45$).[29] Therefore, in terms of light outcoupling effects, replacing ITO ($n = 2.10$) with Ormocomp® ($n = 1.52$) leads to an improved refractive index matching and more light can be extracted from the device.[30] Optical out-coupling is an important factor of the efficiency (η_{ext}) of an OLED, as the efficiency can be described by

$$\eta_{ext}(\lambda) = \eta_{int}(\lambda)\eta_c(\lambda). \quad (1)$$

External quantum efficiency (η_{ext}), equals the internal quantum efficiency (η_{int}) times fraction of out-coupled light (η_c).[31] Considering the device geometry as depicted in Figures 1(a) and 1(b), light out-coupling was calculated for normal incident light at 450 nm, with the transfer matrix

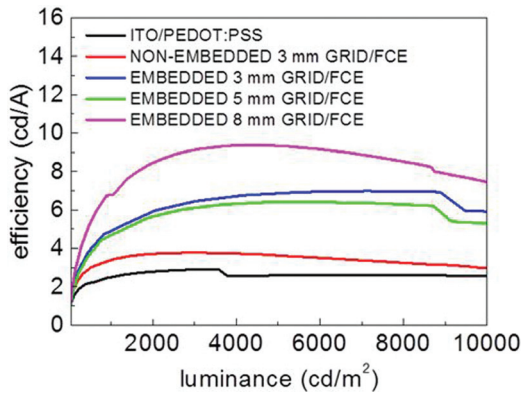

FIG. 3. Current efficiencies of PLEDs on tested electrode stacks.

method. As an approximation, the Ca/Al layer was not considered in the simulation because it was identical for both stacks. The simulation showed that the ITO device stack has a transmittance of 80%, while the grid device has a transmittance of 99% (grid lines are not accounted for). In the following, we assume that both devices have a similar η_{int} as all have the same cathode layer and light emitting layer stack and are operated at comparable current densities. According to (1), this leads to an improved efficiency (η_{ext}) (shadowing and electrical losses not accounted for) of 22% for light coupled out under normal incidence.

Yet, to explain the observation of a 250% improvement in efficiency, light coupled into the substrate as well as into waveguide modes has also to be taken into account. Typically the percentage of the internally generated light coupled into waveguide modes, into the substrate, and into plasmonic as well as other electrical loss modes is of a similar order of magnitude, if not greater, as the percentage of outcoupled light.[32–34] Therefore, if these loss channels are no longer active and since the calculated out-coupling factor $\eta_c(\lambda)$ for normal incident light is close to 99%, it is reasonable to assume that in this modified device stack also light otherwise lost into waveguide modes and substrate modes can be coupled out of the device to yield the observed overall increase in the device efficiency.

The PLEDs on embedded grid/PEDOT:PSS stacks with 3 mm and 5 mm exhibit efficiencies of up to 7 and 6.4 cd/A, respectively. This further increase in efficiency from 3 mm non-embedded to 3 mm and 5 mm embedded grids is not only explained by the reduction of the leakage currents by embedding (see Figure 2(b)) but also by further enhanced light out coupling, as the embedded 3 mm grid devices show a significantly higher 40 000 cd/m^2 at 6500 A/m^2 instead of 12 000 cd/m^2 with the non-embedded 3 mm grid device.

Finally, PLEDs on the 8 mm grid/PEDOT:PSS electrode have the most optimized grid geometry (see Figure S10 of supplementary material) and exhibit an outstanding high efficiency of up to 9.4 cd/A. Fewer remaining grid lines cross the active areas in the 8 mm grid, which additionally reduces remaining shunt losses and significantly reduces light blocking. The 8 mm grid devices also show comparable luminescence values to the ITO reference device in the range of 20 000 cd/m^2.

Table I compares and summarizes the main facts of PLEDs built on embedded and non-embedded honeycomb Ag-grid/PEDOT:PSS electrodes. We note that non-embedded honeycomb grids show very low yield and stability, especially for high voltages. The numbers of the working devices are just

shown for relevant comparison. The numbers clearly illustrate the importance of the embedding process for IJP metal grids related to PLED applications. Efficiency values of ITO and non-embedded grids are in the same range. Embedding of the 3 mm grid leads to a doubled efficiency caused by a higher luminance (22% higher light out-coupling) at constant current, as shown in the column luminance. Due to a further optimized geometry, the device on the embedded 8 mm grid shows the highest efficiency as explained above in the text.

In conclusion, we have developed an IJP embedded Ag-PEDOT:PSS electrode process for highly efficient ITO-free blue polymer light emitting diodes. Although at low yields, non-embedded grids can show similar performance to the ITO reference. The developed embedding process for IJP grid/PEDOT:PSS electrodes can be used to achieve intimate surface/interfaces for PLEDs. The proposed embedding process for ITO-free PLEDs, together with the optimized honeycomb diameter and the flattened topography, led to a significant improvement of the device performance via enhanced light outcoupling effects, due to better refractive index matching of the Ormocomp® embedding material compared to ITO. An overall increase in the efficiency of 250% compared to the ITO reference device was achieved with the 8 mm embedded grid/PEDOT:PSS device, because of embedding, enhanced light out coupling, and optimized grid geometry. For upscaling of the process, several printing processes are feasible. In case a variable device design is required, IJP may also be used in an upscaling of the process, for high throughput production the grid printing will need to be transferred to a flexo- or screen printing process. First experiments also show that the embedding process can be scaled to larger area substrates in the range of 15 cm × 15 cm, which also makes it feasible to work on an industrial scale fabrication process in the next step targeting even larger device areas.

See supplementary material for the detailed description of the fabrication and characterization methods. Profilometer measurements of the IJP lines are given in Figures S1–S4. Figure S5 shows the transmission of the Ag-grids on glass and ITO on glass. Figures S6–S9 display the electroluminescence spectra of the various devices. Figure S10 shows the results of an approximate calculation of the losses in a grid device in terms of spacing.

The authors acknowledge the financial contribution of Plasmas project: Grant Agreement No.: 604568, Call (part) identifier: FP7-NMP-2013-SME-7.

The authors thank Merck KGaA for providing the light emitting polymers.

[1]C. W. Tang and S. A. Van Slyke, Appl. Phys. Lett. **51**, 913 (1987).
[2]J. H. Burroughes, D. D. C. Bradley, A. R. Brown, R. N. Marks, K. MacKay, R. H. Friend, P. L. Burns, and A. B. Holmes, Nature **347**, 539 (1990).
[3]M. Eritt, C. May, K. Leo, M. Toerker, and C. Radehaus, Thin Solid Films **518**, 3042 (2010).
[4]B. Zimmermann, M. Glatthaar, M. Niggemann, M. K. Riede, A. Hinsch, and A. Gombert, Sol. Energy Mater. Sol. Cells **91**, 374 (2007).
[5]S. De, T. M. Higgins, P. E. Lyons, E. M. Doherty, P. N. Nirmalraj, W. J. Blau, J. J. Boland, and J. N. Coleman, ACS Nano **3**, 1767 (2009).
[6]W. Gaynor, G. F. Burkhard, M. D. McGehee, and P. Peumans, Adv. Mater. **23**, 2905 (2011).
[7]Y. S. Kim, M. H. Chang, E. J. Lee, D. W. Ihm, and J. Y. Kim, Synth. Met. **195**, 69 (2014).
[8]J. Y. Lee, S. T. Connor, Y. Cui, and P. Peumans, Nano Lett. **8**, 689 (2008).
[9]S. Choi, S.-J. Kim, C. Fuentes-Hernandez, and B. Kippelen, Opt. Express **19**(Suppl 4), A793 (2011).
[10]Y. Galagan, B. Zimmermann, E. W. C. Coenen, M. Jørgensen, D. M. Tanenbaum, F. C. Krebs, H. Gorter, S. Sabik, L. H. Slooff, S. C. Veenstra, J. M. Kroon, and R. Andriessen, Adv. Energy Mater. **2**, 103–110 (2012).
[11]D. S. Ghosh, T. L. Chen, and V. Pruneri, Appl. Phys. Lett. **96**, 2008 (2010).
[12]Y. Jang, J. Kim, and D. Byun, J. Phys. D: Appl. Phys. **46**, 155103 (2013).
[13]L. Zhou, H. Y. Xiang, S. Shen, Y. Q. Li, J. De Chen, H. J. Xie, and J. X. Tang, "High-performance flexible organic light-emitting diodes using embedded silver network transparent electrodes," ACS Nano **8**(12), 12796–12805 (2014).
[14]K. Peng, Y. Ho, D. Wei, Y. Yu, and Y. Yao, Org. Electron. **15**, 3043 (2014).
[15]F. L. M. Sam, M. A. Razali, K. D. G. I. Jayawardena, C. A. Mills, L. J. Rozanski, M. J. Beliatis, and S. R. P. Silva, Org. Electron. **15**, 3492 (2014).
[16]M. Slawinski, M. Weingarten, M. Heuken, A. Vescan, and H. Kalisch, Org. Electron. Phys. Mater. Appl. **14**, 2387 (2013).
[17]J. Van Deelen, H. Rendering, H. Het Mannetje, L. Klerk, and A. Hovestad, Conf. Rec. IEEE Photovoltaic Spec. Conf. **1**, 2003 (2012).
[18]S. Jung, S. Lee, M. Song, D.-G. Kim, D. S. You, J.-K. Kim, C. S. Kim, T.-M. Kim, K.-H. Kim, J.-J. Kim, and J.-W. Kang, "Extremely flexible transparent conducting electrodes for organic devices," Adv. Energy Mater. **4**(1), 1300474 (2014)..
[19]O. Glushko, A. Klug, E. J. W. List-Kratochvil, and M. J. Cordill, "Relationship between mechanical damage and electrical degradation in polymer-supported metal films subjected to cyclic loading," Mater. Sci. Eng. A **662**, 157–161 (2016).
[20]C. K. Cho, W. J. Hwang, K. Eun, S. H. Choa, S. I. Na, and H. K. Kim, "Mechanical flexibility of transparent PEDOT:PSS electrodes prepared by gravure printing for flexible organic solar cells," Sol. Energy Mater. Sol. Cells **95**(12), 3269–3275 (2011).
[21]B. J. de Gans, P. C. Duineveld, and U. S. Schubert, Adv. Mater. **16**, 203 (2004).
[22]J. Schneider, P. Rohner, D. Thureja, M. Schmid, P. Galliker, and D. Poulikakos, Adv. Funct. Mater. **26**, 833 (2016).
[23]F. Hermerschmidt, I. Burgués-Ceballos, A. Savva, E. D. Sepos, A. Lange, C. Boeffel, S. Nau, E. J. List-Kratochvil, and S. A. Choulis, "High performance indium tin oxide-free solution-processed organic light emitting diodes based on inkjet-printed fine Ag grid lines," Flexible Printed Electron. **1**(3), 35004 (2016).
[24]I. Burgués-Ceballos, N. Kehagias, C. M. Sotomayor-Torres, M. Campoy-Quiles, and P. D. Lacharmoise, Sol. Energy Mater. Sol. Cells **127**, 50 (2014).
[25]S. Nau, N. Schulte, S. Winkler, J. Frisch, A. Vollmer, N. Koch, S. Sax, and E. J. W. List, Adv. Mater. **25**, 4420 (2013).
[26]Y. H. Kim, J. Lee, W. M. Kim, C. Fuchs, S. Hofmann, H. W. Chang, M. C. Gather, L. Müller-Meskamp, and K. Leo, "We want our photons back: Simple nanostructures for white organic light-emitting diode outcoupling," Adv. Funct. Mater. **24**(17), 2553–2559 (2014).
[27]Y. H. Kim, J. Lee, S. Hofmann, M. C. Gather, L. Müller-Meskamp, and K. Leo, "Achieving high efficiency and improved stability in ITO-free transparent organic light-emitting diodes with conductive polymer electrodes," Adv. Funct. Mater. **23**(30), 3763–3769 (2013).
[28]C. Wu, "Exploring full potential of conducting polymers for enhancing light out-coupling of OLEDs," in *Light, Energy and the Environment 2015* (Optical Society of America, 2015), paper DTu2D.1.
[29]Y. Sun and S. R. Forrest, "Enhanced light out-coupling of organic light-emitting devices using embedded low-index grids," Nat. Photonics **2**, 483–487 (2008).
[30]T. Tsutsui, M. Yahiro, H. Yokogawa, K. Kawano, and M. Yokoyama, "Doubling coupling-out efficiency in organic light-emitting devices using a thin silica aerogel layer," Adv. Mater. **13**(15), 1149–1152.
[31]S. R. Forrest, D. D. C. Bradley, and M. E. Thompson, "Measuring the efficiency of organic light-emitting devices," Adv. Mater. **15**(13), 1043–1048 (2003).
[32]R. Meerheim, M. Furno, S. Hofmann, B. Lüssem, and K. Leo, Appl. Phys. Lett. **97**, 253305 (2010).
[33]S. Nowy, B. C. Krummacher, J. Frischeisen, N. A. Reinke, and W. Brütting, J. Appl. Phys. **104**, 123109 (2008).
[34]S. Reineke, M. Thomschke, B. Lüssem, and K. Leo, Rev. Mod. Phys. **85**, 1245 (2013).